Electronic Supplementary Material (ESI) for Materials Chemistry Frontiers.
This journal is © the Partner Organisations 2024

Supporting Information

Developing Piezochromic Luminescent Materials via Regioselective Cyanation of Naphthalimide-Cyanostilbene Derivatives

Hao Jia,[‡a] Xuening Sun,[‡c] Xinmiao Meng,[a] Min Wu,[a] Aisen Li,[a] Miao Yang,[b] Chengyuan Wang,*[b] Jiaxiang Yang,*[b] Kai Wang,[a] Qian Li,*[a] and Lei Li*[a]

[a.] School of Physics Science and Information Technology, Shandong Key Laboratory of Optical Communication Science and Technology, Liaocheng University, Liaocheng 25200, China.
E-mail: liqian@lcu.edu.cn, leili@lcu.edu.cn

[b.] School of Chemistry and Chemical Engineering, Key Laboratory of Structure and Functional Regulation of Hybrid Materials of Ministry of Education, Anhui University, Hefei 230601, China.
E-mail: chengyuan.wang@ahu.edu.cn, jxyang@ahu.edu.cn

[c.] State Key Laboratory of Superhard Materials, College of Physics, Jilin University, Changchun 130012, China.

‡ These authors have contributed equally to this work.

* Corresponding authors.
E-mail addresses:
chengyuan.wang@ahu.edu.cn (C. Wang)
jxyang@ahu.edu.cn (J. Yang)
liqian@lcu.edu.cn (Q. Li)
leili@lcu.edu.cn (L. Li)

Experimental Details

Sample preparation

All the chemicals used in this work are purchased from commercial suppliers without purification. Analytical nuclear magnetic resonance (NMR) spectra were recorded on Bruker AVANCE NEO 500, at a constant temperature of 298 K. Chemical shifts are reported in δ values in ppm using tetramethylsilane (TMS) or residual solvent as internal standard and coupling constants (*J*) are denoted in Hz. Multiplicities are denoted as follows: s = singlet, d = doublet, t = triplet, dd = double doublet and m = multiplet. The detailed synthesized methods are shown below:

NICNα-R (R = 1C, 2C, 3C and 4C) were synthesized according to the previous report.[1] The intermediate compound **5** (1.40 mmol) and compound **2** (1.68 mmol, R = 1C, 2C, 3C and 4C) were added to the ethanol (80 mL) in a 250 mL round-button flask. The solution was refluxed continuously to dissolve all the precursors. The obtained solution was then added *t*-BuOK (2.80 mmol), and further stirred for 6 h. Finally, the solution was filtrated to achieve the targeted sample. The samples were purified by column chromatography to obtain desired product (petroleum ether: CH_2Cl_2 = 1:3, v/v).

NICNα-1C, light yellow solid, 80% yield. ^{1}H NMR (500 MHz, $CDCl_3$, ppm) *δ*: 8.64 (d, *J* = 7.5 Hz, 2H), 8.08 (d, *J* = 8.5 Hz, 1H), 7.74 – 7.69 (m, 1H), 7.67 (d, *J* = 7.5 Hz, 1H), 7.54 – 7.49 (m, 2H), 7.48 – 7.44 (m, 2H), 7.35 – 7.31 (m, 2H), 6.92 – 6.88 (m, 2H), 5.34 (s, 1H), 4.25 – 4.19 (m, 2H), 3.82 (s, 3H), 1.78 – 1.71 (m, 2H), 1.51 – 1.43 (m, 2H), 0.99 (t, *J* = 7.5 Hz, 3H). ^{13}C NMR (125 MHz, $CDCl_3$, ppm) *δ*: 13C NMR (126 MHz, Chloroform-d) δ 164.17, 163.97, 160.07, 145.29, 139.21, 135.26, 132.01, 131.25, 131.05, 130.67, 130.29, 129.85, 128.61, 128.34, 127.76, 127.05, 124.81, 123.04, 122.25, 121.66, 114.14, 55.30, 48.22, 40.30, 30.20, 20.38, 13.84.

NICNα-2C, yellow solid, 80% yield. ^{1}H NMR (500 MHz, $CDCl_3$, ppm) *δ*: 8.65 (d, *J* = 7.5 Hz, 2H), 8.10 – 8.07 (m, 1H), 7.72 (dd, *J* = 8.5, 7.2 Hz, 1H), 7.67 (d, *J* = 7.5 Hz, 1H), 7.51 (d, *J* = 8.5 Hz, 2H), 7.46 (d, *J* = 8.5 Hz, 2H), 7.33 – 7.29 (m, 2H), 6.92 – 6.84 (m, 2H), 5.33 (s, 1H), 4.24 – 4.19 (m, 2H), 4.07 – 4.00 (m, 2H), 1.79 – 1.71 (m, 2H), 1.52 – 1.44 (m, 2H), 1.42 (t, *J* = 7.0 Hz, 3H), 1.00 (t, *J* = 7.5 Hz, 3H).
^{13}C NMR (125 MHz, $CDCl_3$, ppm) *δ*: 164.24, 164.03, 161.16, 145.69, 142.56, 139.16, 135.20, 132.23, 131.41, 131.24, 130.74, 130.54, 129.92, 128.71, 127.79, 127.03, 126.12, 126.00, 123.05, 122.13, 118.41, 114.96, 107.56, 63.76, 40.30, 30.22, 20.39, 14.69, 13.84.

NICNα-3C, light yellow solid, 83% yield. ^{1}H NMR (500 MHz, $CDCl_3$, ppm) *δ*: 8.68 – 8.63 (m, 2H), 8.28 – 8.25 (m, 1H), 7.96 – 7.91 (m, 2H), 7.86 – 7.82 (m, 2H), 7.75 – 7.70 (m, 2H), 7.61 – 7.56 (m, 3H), 7.03 – 6.98 (m, 2H), 4.22 (t, *J* = 7.5 Hz, 2H), 4.01 (t, *J* = 6.5 Hz, 2H), 1.90 – 1.81 (m, 2H), 1.79 – 1.71 (m, 2H), 1.52 – 1.43 (m, 2H), 1.07 (t, *J* = 7.5 Hz, 3H), 0.99 (t, *J* = 7.5 Hz, 3H). ^{13}C NMR (125 MHz, $CDCl_3$, ppm) *δ*: 164.24, 164.04, 161.35, 145.70, 142.59, 139.13, 135.20, 132.24, 131.40, 131.25, 130.75, 130.53,

129.91, 128.70, 127.79, 127.03, 126.06, 125.99, 123.03, 122.11, 118.43, 114.97, 107.48, 69.74, 40.30, 30.22, 22.46, 20.39, 13.85, 10.47.

NICNα-4C, yellow solid, 79% yield. ^{1}H NMR (500 MHz, $CDCl_3$, ppm) δ: 8.66 – 8.61 (m, 2H), 8.25 (dd, J = 8.5, 1.0 Hz, 1H), 7.95 – 7.90 (m, 2H), 7.85 – 7.81 (m, 2H), 7.71 (t, J = 7.5 Hz, 2H), 7.60 – 7.56 (m, 3H), 7.01 – 6.96 (m, 2H), 4.20 (t, J = 8.0 Hz, 2H), 4.04 (t, J = 6.5 Hz, 2H), 1.84 – 1.70 (m, 4H), 1.56 – 1.42 (m, 4H), 1.02 – 0.96 (m, 6H). ^{13}C NMR (125 MHz, $CDCl_3$, ppm) δ: 164.17, 163.96, 161.32, 145.63, 142.53, 139.07, 135.14, 132.19, 131.36, 131.19, 130.69, 130.50, 129.84, 128.64, 127.75, 126.98, 126.00, 125.94, 122.97, 122.05, 118.39, 114.92, 107.40, 67.92, 40.25, 31.11, 30.18, 20.36, 19.17, 13.82, 13.79.

NICNβ-1C, ^{1}H NMR (500 MHz, $CDCl_3$, ppm) δ: 8.68 – 8.63 (m, 2H), 8.28 (d, J = 8.5 Hz, 1H), 8.05 (d, J = 8.0 Hz, 2H), 7.76 – 7.71 (m, 2H), 7.69 – 7.65 (m, 2H), 7.63 – 7.60 (m, 2H), 7.54 (s, 1H), 7.02 – 6.98 (m, 2H), 4.25 – 4.20 (m, 2H), 3.88 (s, 3H), 1.79 – 1.72 (m, 2H), 1.48 (h, J = 7.4 Hz, 2H), 1.00 (t, J = 7.5 Hz, 3H). ^{13}C NMR (125 MHz, $CDCl_3$, ppm) δ: 164.17, 163.96, 161.32, 145.63, 142.53, 139.07, 135.14, 132.19, 131.36, 131.19, 130.69, 130.50, 129.84, 128.64, 127.75, 126.98, 126.00, 125.94, 122.97, 122.05, 118.39, 114.92, 107.40, 67.92, 40.25, 31.11, 30.18, 20.36, 19.17, 13.82, 13.79.

NICNβ-2C, ^{1}H NMR (500 MHz, $CDCl_3$, ppm) δ: 8.65 (t, J = 6.5 Hz, 2H), 8.27 (d, J = 8.5 Hz, 1H), 8.03 (d, J = 8.0 Hz, 2H), 7.76 – 7.70 (m, 2H), 7.65 (d, J = 8.0 Hz, 2H), 7.60 (d, J = 7.5 Hz, 2H), 7.52 (s, 1H), 6.98 (d, J = 8.5 Hz, 2H), 4.21 (t, J = 8.0 Hz, 2H), 4.10 (q, J = 7.0 Hz, 2H), 1.79 – 1.71 (m, 2H), 1.51 – 1.42 (m, 5H), 0.99 (t, J = 7.5 Hz, 3H). ^{13}C NMR (125 MHz, $CDCl_3$, ppm) δ: 164.20, 163.99, 160.09, 145.65, 140.40, 138.70, 134.21, 132.22, 131.24, 130.70, 130.41, 129.81, 129.26, 128.68, 127.78, 127.39, 127.06, 126.47, 123.02, 122.18, 118.04, 115.01, 112.36, 63.71, 40.28, 30.20, 20.37, 14.71, 13.83.

NICNβ-3C, ^{1}H NMR (500 MHz, $CDCl_3$, ppm) δ: 8.67 – 8.61 (m, 2H), 8.29 – 8.25 (m, 1H), 8.06 – 8.01 (m, 2H), 7.74 – 7.69 (m, 2H), 7.66 – 7.62 (m, 2H), 7.62 – 7.58 (m, 2H), 7.52 (s, 1H), 7.00 – 6.95 (m, 2H), 4.24 – 4.18 (m, 2H), 4.00 – 3.95 (m, 2H), 1.89 – 1.80 (m, 2H), 1.78 – 1.71 (m, 2H), 1.51 – 1.43 (, 2H), 1.06 (t, J = 7.5 Hz, 3H), 0.99 (t, J = 7.5 Hz, 3H). ^{13}C NMR (125 MHz, $CDCl_3$, ppm) δ: 164.16, 163.96, 160.28, 145.62, 140.36, 138.63, 134.20, 132.20, 131.21, 130.68, 130.39, 129.78, 129.24, 128.66, 127.76, 127.35, 127.04, 126.39, 123.00, 122.15, 118.03, 115.02, 112.34, 69.71, 40.26, 30.19, 22.48, 20.36, 13.82, 10.45.

NICNβ-4C, ^{1}H NMR (500 MHz, $CDCl_3$, ppm) δ: 8.67 – 8.62 (m, 2H), 8.27 (d, J = 8.5 Hz, 1H), 8.04 (d, J = 8.0 Hz, 2H), 7.75 – 7.70 (m, 2H), 7.67 – 7.63 (m, 2H), 7.60 (d, J = 8.0 Hz, 2H), 7.52 (s, 1H), 7.00 – 6.96 (m, 2H), 4.22 (t, J = 7.5 Hz,, 2H), 4.03 (t, J = 6.5 Hz, 2H), 1.84 – 1.71 (m, 4H), 1.56 – 1.43 (m, 4H), 1.02 – 0.97 (m, 6H). ^{13}C NMR (125 MHz, $CDCl_3$, ppm) δ: 164.21, 164.00, 160.32, 145.66, 140.40, 138.67, 134.23, 132.23, 131.25, 130.71, 130.42, 129.83, 129.26, 128.69, 127.79, 127.38, 127.06, 126.41, 123.03, 122.19, 118.06, 115.04, 112.39, 67.95, 40.29, 31.20, 30.21, 20.38, 19.20, 13.83, 13.81.

NICNβ-R (R = 1C, 2C, 3C and 4C) were synthesized with the similar method based on the previous report.[1]

Data analyses

The lattice parameters are obtained via Pawley refinements of ADXRD patterns with the software of Material Studio. The IR modes are also calculated via this software. The Hirshfeld surface is calculated using the software CrystalExplorer.

The pressure-volume (*P*-*V*) data were fitted by the third-order Birch-Murnaghan (B-M) equation of state:

$$P(V) = \frac{3B_0}{2}\left[\left(\frac{V_0}{V}\right)^{\frac{7}{3}} - \left(\frac{V_0}{V}\right)^{\frac{5}{3}}\right] \times \left\{1 + \frac{3}{4}\left(B_0' - 4\right)\left[\left(\frac{V_0}{V}\right)^{\frac{2}{3}} - 1\right]\right\}$$

where V_0 is the zero-pressure volume, B_0 is the bulk modulus, and B_0' is a parameter for the pressure derivative.

Table S1. The crystallographic data of NICNα-R (R = 1C, 2C, 3C and 4C).

Identification	**NICNα-1C**	**NICNα-2C**	**NICNα-3C**	**NICNα-4C**
Formula	$C_{32}H_{26}N_2O$	$C_{33}H_{28}N_2O$	$C_{34}H_{30}N_2O_3$	$C_{35}H_{32}N_2O_3$
Formula weight	486.55	500.57	514.60	528.62
Temperature (K)	293	293	293	293
Wavelength (Å)	1.54	1.54	1.54	1.54
Crystal system	triclinic	triclinic	triclinic	triclinic
Space group	*P*-1	*P*-1	*P*-1	*P*-1
***a* (Å)**	9.26	9.21	6.83	6.76
***b* (Å)**	10.86	12.09	14.39	14.32
***c* (Å)**	12.87	12.62	15.09	15.95
***α* (°)**	103.57	105.85	66.16	116.10
***β* (°)**	104.13	110.71	82.27	90.86
***γ* (°)**	97.04	91.75	84.89	94.70
Volume	1198.64	1250.47	1343.68	1379.78
Z	2	2	2	2
Density (g/cm^3)	1.35	1.33	1.27	1.27
Absorption coefficient (mm^{-1})	0.69	0.68	0.65	0.64
***F* (000)**	512	528	544	560
_reflns_number_gt	3856	3681	3641	3910

_reflns_number_total	4269	4540	4518	4624
***R*_factor_all**	0.05	0.06	0.06	0.05
***wR*_factor_ref**	0.12	0.13	0.16	0.12

Table S2. The detailed atomic positions in NICNα-1C.

Atom	**x/a**	**y/b**	**z/c**
O001	0.04	-0.41	0.41
O002	-0.32	-0.22	0.53
O003	1.31	1.01	0.97
N004	-0.13	-0.32	0.48
C005	0.01	-0.32	0.47
C006	0.13	-0.21	0.54
C007	0.69	0.29	0.73
H007	0.75	0.32	0.69
C008	0.20	0.02	0.66
C009	0.58	0.17	0.68
H009	0.57	0.13	0.60
C00A	0.09	-0.10	0.60
C00B	0.70	0.36	0.84
C00C	-0.06	-0.10	0.60
C00D	1.01	0.66	0.89
C00E	0.15	0.13	0.72
H00E	0.22	0.20	0.75
N00F	0.76	0.60	1.08
C00G	0.48	0.13	0.73
C00H	0.91	0.54	0.85
H00H	0.91	0.48	0.79
C00I	0.80	0.48	0.89
C00J	0.36	0.01	0.67
C00K	0.50	0.19	0.84
H00K	0.44	0.16	0.88
C00L	0.39	-0.10	0.61

H00L	0.49	-0.10	0.62
C00M	0.60	0.30	0.90
H00M	0.61	0.35	0.97
C00N	0.78	0.55	1.00
C00O	0.28	-0.21	0.55
H00O	0.31	-0.28	0.51
C00P	-0.18	-0.21	0.54
C00Q	0.00	0.12	0.71
H00Q	-0.03	0.20	0.74
C00R	-0.11	0.01	0.65
H00R	-0.21	0.01	0.65
C00S	-0.25	-0.44	0.43
H00A	-0.32	-0.45	0.47
H00B	-0.20	-0.51	0.42
C00T	1.21	0.90	0.95
C00U	-0.34	-0.44	0.31
H00C	-0.27	-0.43	0.27
H00D	-0.39	-0.37	0.31
C00V	1.19	0.81	0.85
H00V	1.25	0.83	0.80
C00W	1.09	0.69	0.82
H00W	1.08	0.63	0.75
C00X	1.12	0.87	1.02
H00X	1.13	0.94	1.08
C00Y	1.02	0.76	0.99
H00Y	0.97	0.74	1.04
C00Z	-0.45	-0.57	0.25
H00F	-0.50	-0.57	0.18
H00G	-0.40	-0.64	0.25
C010	-0.57	-0.60	0.31
H01A	-0.64	-0.67	0.27
H01B	-0.61	-0.52	0.33
H01C	-0.52	-0.61	0.38

C011	1.34	1.10	1.08
H01D	1.42	1.17	1.08
H01E	1.37	1.06	1.13
H01F	1.25	1.13	1.08

Table S3. The detailed atomic positions in NICNα-2C.

Atom	**x/a**	**y/b**	**z/c**
O001	0.09	-0.37	0.45
O002	-0.28	-0.19	0.57
O003	1.24	0.96	0.96
N004	-0.09	-0.28	0.52
C005	0.17	-0.17	0.57
C006	0.11	-0.07	0.62
C007	-0.04	-0.07	0.62
C008	0.49	0.15	0.73
C009	0.57	0.19	0.67
H009	0.56	0.14	0.60
C00A	0.69	0.36	0.84
C00B	-0.15	-0.18	0.57
C00C	0.67	0.29	0.72
H00C	0.73	0.31	0.68
C00D	0.15	0.14	0.71
H00D	0.22	0.21	0.74
C00E	0.97	0.64	0.88
C00F	0.06	-0.28	0.51
C00G	0.79	0.48	0.89
C00H	0.22	0.04	0.67
C00I	-0.09	0.03	0.66
H00I	-0.20	0.03	0.66
C00J	0.32	-0.16	0.57
H00J	0.35	-0.23	0.54
N00K	0.76	0.60	1.08

C00L	1.15	0.85	0.94
C00M	0.00	0.14	0.71
H00M	-0.04	0.20	0.74
C00N	0.37	0.04	0.68
C00O	0.88	0.52	0.84
H00O	0.88	0.47	0.77
C00P	-0.19	-0.39	0.47
H00A	-0.26	-0.39	0.52
H00B	-0.13	-0.46	0.49
C00Q	0.51	0.22	0.85
H00Q	0.46	0.20	0.89
C00R	0.42	-0.06	0.63
H00R	0.52	-0.06	0.63
C00S	0.61	0.33	0.90
H00S	0.63	0.37	0.97
C00T	1.14	0.77	0.84
H00T	1.18	0.78	0.79
C00U	0.78	0.55	1.00
C00V	0.99	0.73	0.98
H00V	0.94	0.72	1.03
C00W	-0.29	-0.42	0.34
H00E	-0.22	-0.42	0.30
H00F	-0.36	-0.37	0.33
C00X	1.05	0.66	0.81
H00X	1.04	0.60	0.74
C00Y	1.08	0.83	1.01
H00Y	1.09	0.89	1.08
C00Z	-0.39	-0.54	0.29
H00G	-0.45	-0.56	0.21
H00H	-0.31	-0.60	0.30
C010	-0.50	-0.56	0.35
H01A	-0.56	-0.64	0.31
H01B	-0.56	-0.50	0.36

H01C	-0.43	-0.57	0.43
C011	1.29	1.04	1.08
H01D	1.34	1.00	1.14
H01E	1.19	1.07	1.09
C012	1.40	1.14	1.08
H01F	1.34	1.18	1.03
H01G	1.48	1.11	1.07
H01H	1.43	1.19	1.16

Table S4. The detailed atomic positions in NICNα-3C.

Atom	**x/a**	**y/b**	**z/c**
O001	0.25	0.40	1.05
O002	0.21	1.15	-0.20
O003	0.34	0.84	-0.20
N004	0.27	0.99	-0.20
C005	0.25	1.02	-0.04
C006	0.28	0.87	0.11
C007	0.22	0.44	0.95
C008	0.28	0.91	0.01
C009	0.21	0.52	0.75
C00A	0.22	1.08	0.01
H00A	0.20	1.15	-0.03
C00B	0.32	0.85	-0.04
N00C	0.72	0.58	0.62
C00D	0.34	0.63	0.47
C00E	0.34	0.56	0.80
H00E	0.42	0.61	0.76
C00F	0.33	0.72	0.27
C00G	0.20	0.56	0.65
H00G	0.08	0.56	0.63
C00H	0.25	0.94	0.16
H00H	0.25	0.91	0.23

C00I	0.36	0.59	0.58
C00J	0.51	0.64	0.41
H00J	0.63	0.62	0.43
C00K	0.34	0.52	0.89
H00K	0.43	0.55	0.92
C00L	0.32	0.76	0.16
C00M	0.50	0.68	0.31
H00M	0.62	0.68	0.27
C00N	0.24	1.06	-0.15
C00O	0.16	0.67	0.43
H00O	0.05	0.67	0.47
C00P	0.09	0.45	0.81
H00P	0.00	0.42	0.79
C00Q	0.09	0.40	0.91
H00Q	0.01	0.35	0.95
C00R	0.31	0.89	-0.15
C00S	0.36	0.74	0.01
H00S	0.39	0.70	-0.03
C00T	0.16	0.71	0.33
H00T	0.03	0.74	0.31
C00U	0.22	1.04	0.11
H00U	0.20	1.08	0.14
C00V	0.37	0.70	0.11
H00V	0.40	0.64	0.14
C00W	0.56	0.59	0.60
C00X	0.13	0.32	1.12
H00B	0.16	0.26	1.10
H00C	-0.01	0.34	1.12
C00Y	0.20	0.29	1.22
H00D	0.18	0.35	1.23
H00F	0.34	0.27	1.22
C00Z	0.25	1.03	-0.30
H00I	0.15	1.09	-0.32

H00L	0.20	0.98	-0.32
C010	0.44	1.07	-0.37
H01A	0.49	1.12	-0.35
H01B	0.54	1.02	-0.36
C011	0.08	0.21	1.30
H01C	0.12	0.15	1.29
H01D	-0.06	0.22	1.29
H01E	0.11	0.20	1.36
C012	0.41	1.12	-0.47
H01F	0.33	1.19	-0.48
H01G	0.34	1.08	-0.49
C013	0.60	1.15	-0.54
H01H	0.57	1.17	-0.61
H01I	0.69	1.09	-0.53
H01J	0.67	1.20	-0.53

Table S5. The detailed atomic positions in NICNα-4C.

Atom	**x/a**	**y/b**	**z/c**
O001	0.24	0.05	-0.02
O002	0.22	0.56	1.20
O003	0.37	0.85	1.17
N004	0.28	0.70	1.18
C005	0.28	0.52	0.89
C006	0.24	0.41	0.85
H006	0.24	0.37	0.79
N007	0.73	0.30	0.38
C008	0.37	0.33	0.43
C009	0.22	0.23	0.27
C00A	0.25	0.53	1.05
C00B	0.33	0.69	1.03
C00C	0.28	0.58	0.99
C00D	0.37	0.68	0.87

H00D	0.40	0.71	0.84
C00E	0.21	0.30	0.37
H00E	0.09	0.32	0.39
C00F	0.34	0.09	0.13
H00F	0.42	0.04	0.11
C00G	0.33	0.51	0.73
C00H	0.37	0.74	0.97
H00H	0.40	0.81	1.00
C00I	0.35	0.40	0.53
C00J	0.25	0.60	1.15
C00K	0.52	0.45	0.59
H00K	0.64	0.45	0.56
C00L	0.51	0.51	0.69
H00L	0.62	0.55	0.72
C00M	0.32	0.57	0.83
C00N	0.33	0.76	1.13
C00O	0.17	0.40	0.57
H00O	0.05	0.37	0.54
C00P	0.22	0.11	0.07
C00Q	0.22	0.43	1.01
H00Q	0.20	0.39	1.05
C00R	0.21	0.37	0.91
H00R	0.19	0.29	0.88
C00S	0.16	0.46	0.67
H00S	0.03	0.46	0.70
C00T	0.34	0.15	0.23
H00T	0.42	0.14	0.26
C00U	0.10	0.19	0.11
H00U	0.02	0.21	0.07
C00V	0.09	0.25	0.20
H00V	0.01	0.30	0.23
C00W	0.56	0.31	0.40
C00X	0.13	0.08	-0.09

H00A	0.17	0.15	-0.07
H00B	-0.01	0.07	-0.08
C00Y	0.18	0.01	-0.19
H00C	0.15	-0.06	-0.20
H00G	0.32	0.02	-0.19
C00Z	0.08	0.03	-0.26
H00I	-0.06	0.02	-0.26
H00J	0.11	0.10	-0.25
C010	0.47	0.78	1.34
H01A	0.57	0.82	1.32
H01B	0.52	0.71	1.32
C011	0.27	0.77	1.29
H01C	0.17	0.73	1.31
H01D	0.23	0.83	1.30
C012	0.46	0.84	1.44
H01E	0.39	0.91	1.46
H01F	0.37	0.80	1.47
C013	0.13	-0.04	-0.36
H01G	0.07	-0.02	-0.40
H01H	0.10	-0.11	-0.37
H01I	0.28	-0.03	-0.36
C014	0.66	0.87	1.50
H01J	0.74	0.92	1.48
H01K	0.72	0.81	1.48
H01L	0.64	0.91	1.56

Table S6. The torsion angles between NI and CNα units and the angles between the two benzenic rings within the CNα units for NICNα-R.

Torsion angles	**NICNα-1C**	**NICNα-2C**	**NICNα-3C**	**NICNα-4C**
Between NI-CNα	51.4°	49.9°	68.7°	67.8°
Within CNα	10.6°	8.6°	54.7°	56.4°

Table S7. Comparisons of the pressure-induced emission shifts in typical PCMs.

Compound	**Shift range (nm)**	**Pressure range (GPa)**	**Pressure coefficients (nm/GPa)**	**Refs.**
1,4-Bis[(4-methyloxyphenyl)-1,3,4-oxadiazolyl]- 2,5-bisheptyloxyphenylene	57	9.6	5.9	[2]
Tetraphenylethene	40	10	4.0	[3]
Benzothiazole-enamido boron difluoride complexes	113	10.8	10.5	[4]
Benzothiazole-enamido boron difluoride complexes	125	10.34	12.1	[4]
Triphenylacrylonitrile derivative/(TPAN-MeO-BCrys)	82	10.2	8.0	[5]
Triphenylacrylonitrile derivative/(TPAN-MeO-SCrys)	56	12.3	4.6	[5]
Spiropyrans-pyrene/(SP–Pyr)	100	11.1	9.0	[6]
Cyano-substituted oligo(*p*-phenylene vinylene)derivatives / (mF-TPA)	146	10.1	14.5	[7]
4-(2-(4'-(Diphenylamino)-[1,1'-biphenyl]-4-yl)-1Hphenanthro[9,10-d]imidazol-1-yl)benzonitrile	130	13.2	9.9	[8]
Pyrene-rhodamine B / (PyB)	130	9.0	14.5	[9]
2,6-di(triphenylamine)-4-carbonitrile	113	9.9	11.4	[10]
Truxene	120	11.8	10.2	[11]
9-(1,2,2-triphenylvinyl)anthracene	83	12.9	6.4	[12]
9-(4-(1,2,2-triphenylvinyl)phenyl)anthracene	104	12.5	8.3	[12]

Table S8. The torsion angles between NI and CNβ units and the angles between the two benzenic rings within the CNβ units for NICNβ-R. There are slight differences between our results and the previous reports, which should be raised from the different measurement methods.

Torsion angles	**NICNβ-1C**	**NICNβ-2C**	**NICNβ-3C**	**NICNβ-4C**
Between NI-CNβ	60.9	39.5	61.4	62.8
Within CNβ	8.7	10.1	49.1	51.2

Table S9. The emission (λ_{em}) and absorption (λ_{abs}) wavelength, as well as the Stokes shifts ($\triangle\lambda$) of NICNβ-R at 1 atm and at ≈10 GPa. Λ_{abs} represents the wavelength of absorption edge. The Stokes shifts at 1 atm and high pressure are estimated based on the λ_{em} and λ_{abs}.

	λ_{em} (1 atm)	**λ_{abs} (1 atm)**	**$\triangle\lambda$ (1 atm)**	**λ_{em} (≈10 GPa)**	**λ_{abs} (≈10 GPa)**	**$\triangle\lambda$ (≈10 GPa)**
NICNβ-1C	499.2 nm	473.5 nm	25.7 nm	691.0 nm	684.8 nm	6.2 nm
NICNβ-2C	546.5 nm	509.3 nm	37.2 nm	751.3 nm	651.2 nm	100.1 nm
NICNβ-3C	489.1 nm	467.9 nm	21.2 nm	685.4 nm	642.4 nm	43.0 nm
NICNβ-4C	496.1 nm	463.9 nm	32.2 nm	675.0 nm	593.7 nm	81.3 nm

NMR Spectra of NICNβ-R (R = 1C, 2C, 3C and 4C)

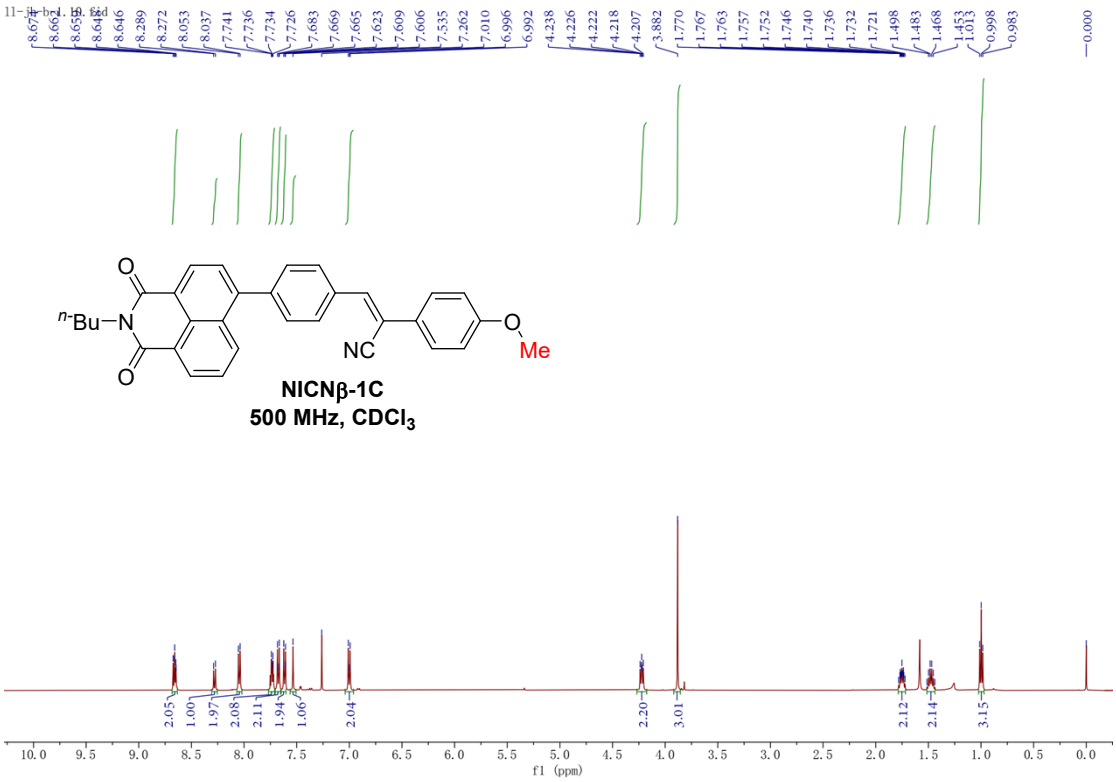

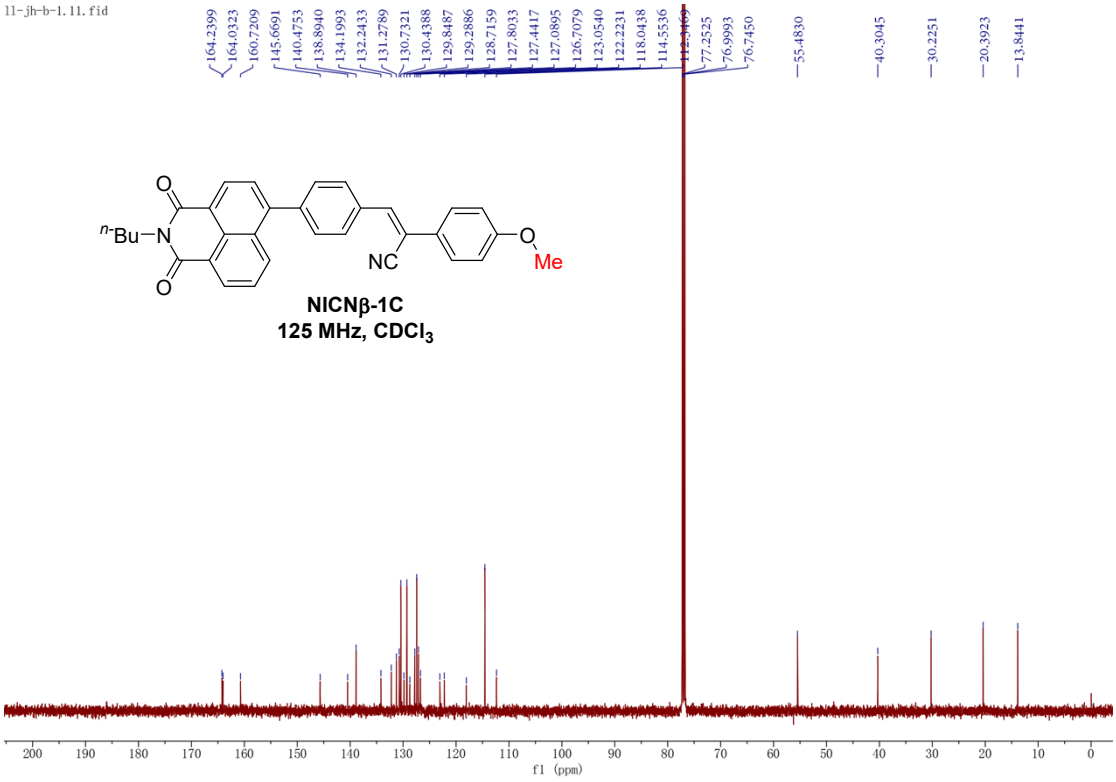

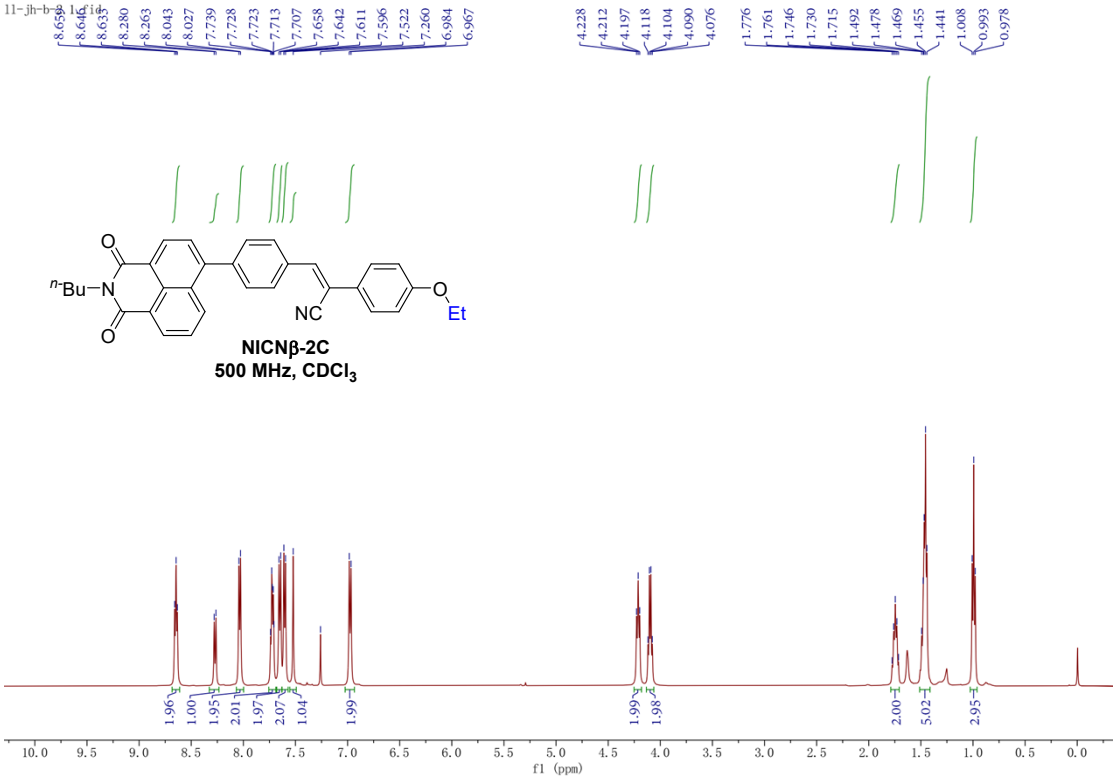

NICNβ-2C
500 MHz, $CDCl_3$

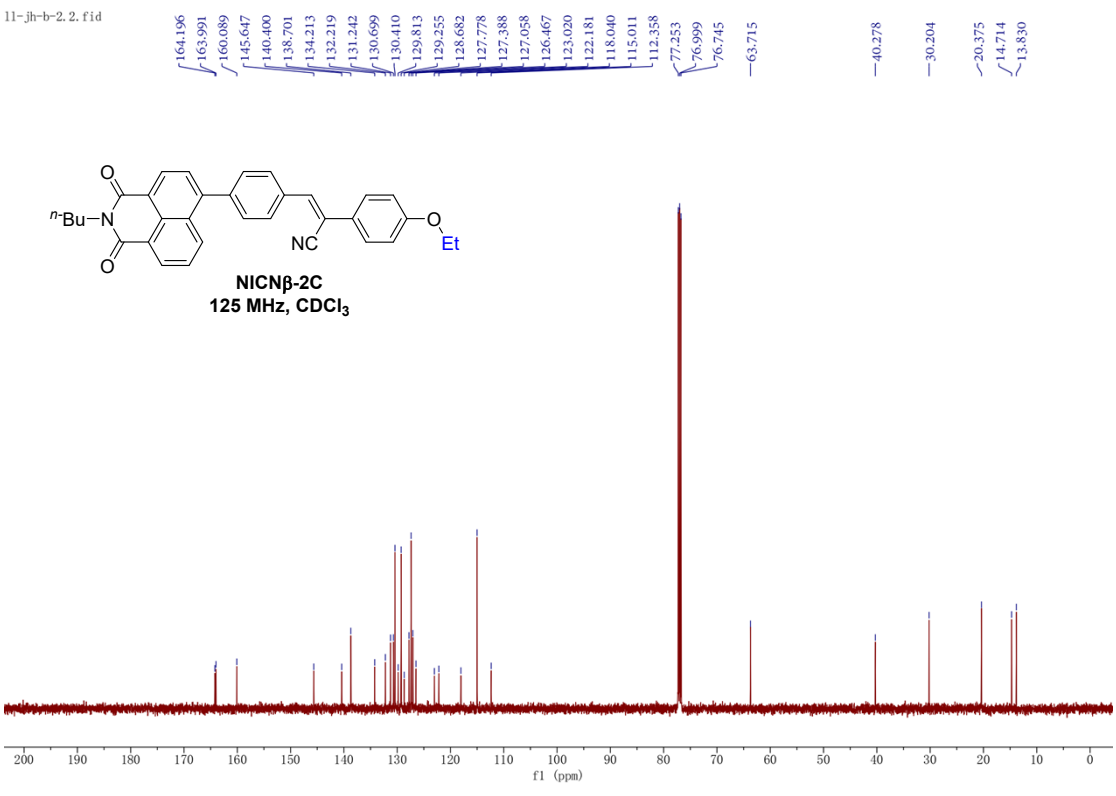

NICNβ-2C
125 MHz, $CDCl_3$

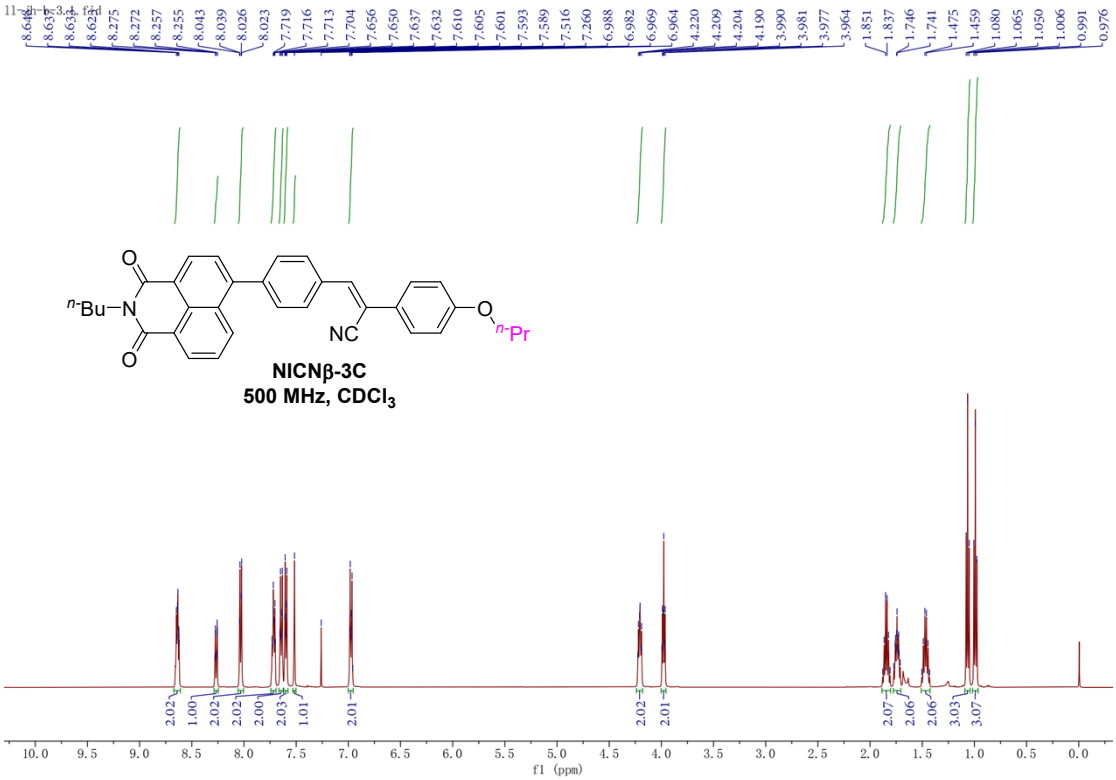

NICNβ-3C
500 MHz, $CDCl_3$

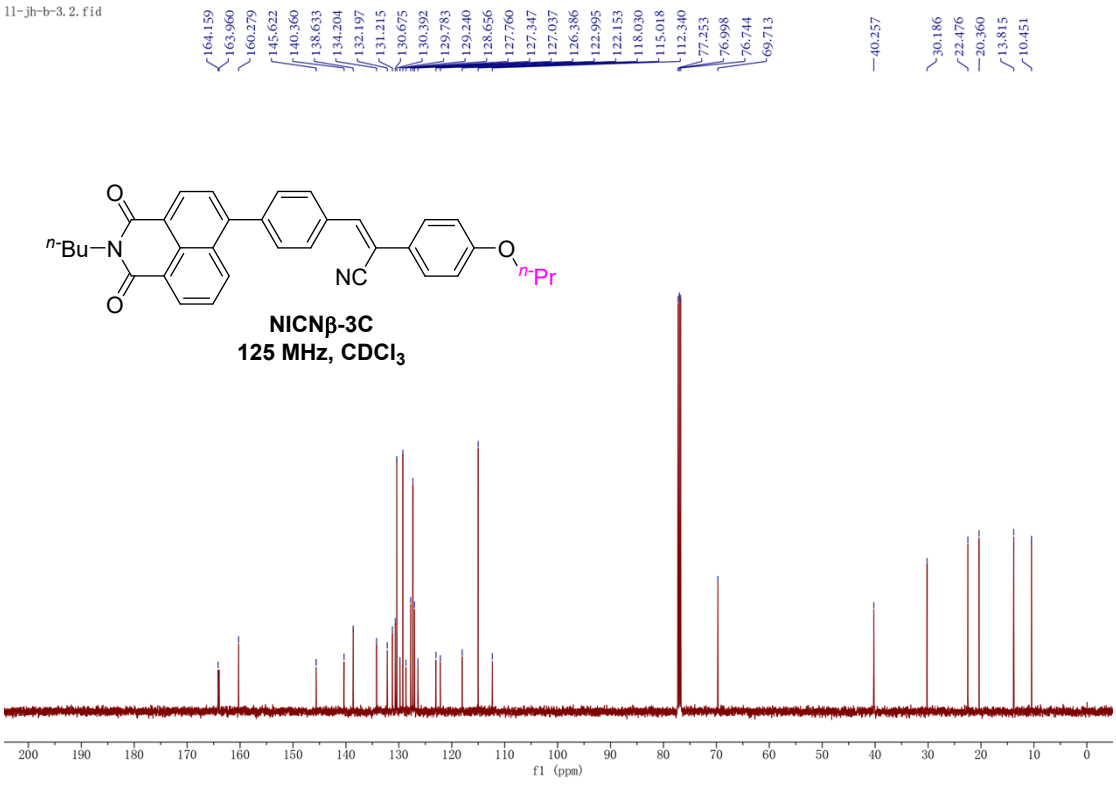

NICNβ-3C
125 MHz, $CDCl_3$

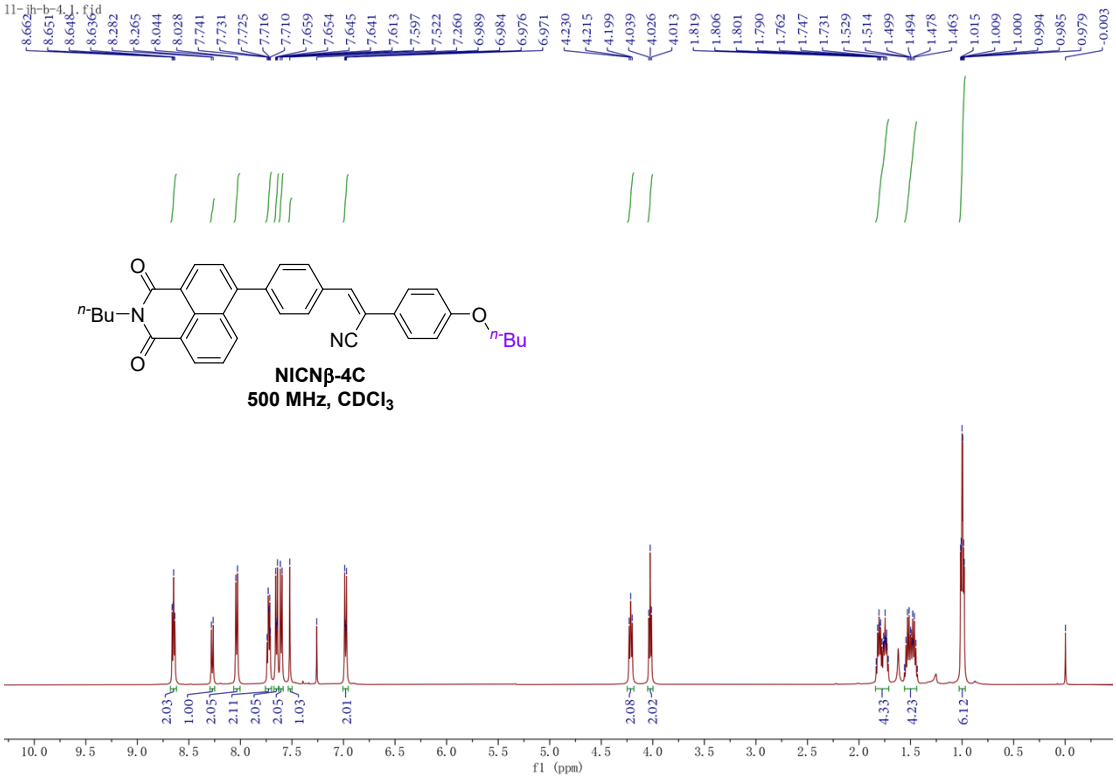
11-jh-b-4.1.fid
8.662
8.651
8.648
8.636
8.282
8.265
8.044
8.028
7.741
7.731
7.725
7.716
7.710
7.659
7.654
7.645
7.641
7.613
7.597
7.522
7.260
6.989
6.984
6.976
6.971
4.230
4.215
4.199
4.039
4.026
4.013
1.819
1.806
1.801
1.790
1.762
1.747
1.731
1.529
1.514
1.499
1.494
1.478
1.463
1.015
1.009
1.000
0.994
0.985
0.979
0.003
O
n-Bu–N
O
NC
O
n-Bu
NICNβ-4C
500 MHz, CDCl3
2.03
1.00
2.05
2.11
2.05
2.05
1.03
2.01
2.08
2.02
4.33
4.23
6.12
10.0
9.5
9.0
8.5
8.0
7.5
7.0
6.5
6.0
5.5
5.0
4.5
4.0
3.5
3.0
2.5
2.0
1.5
1.0
0.5
0.0
f1 (ppm)

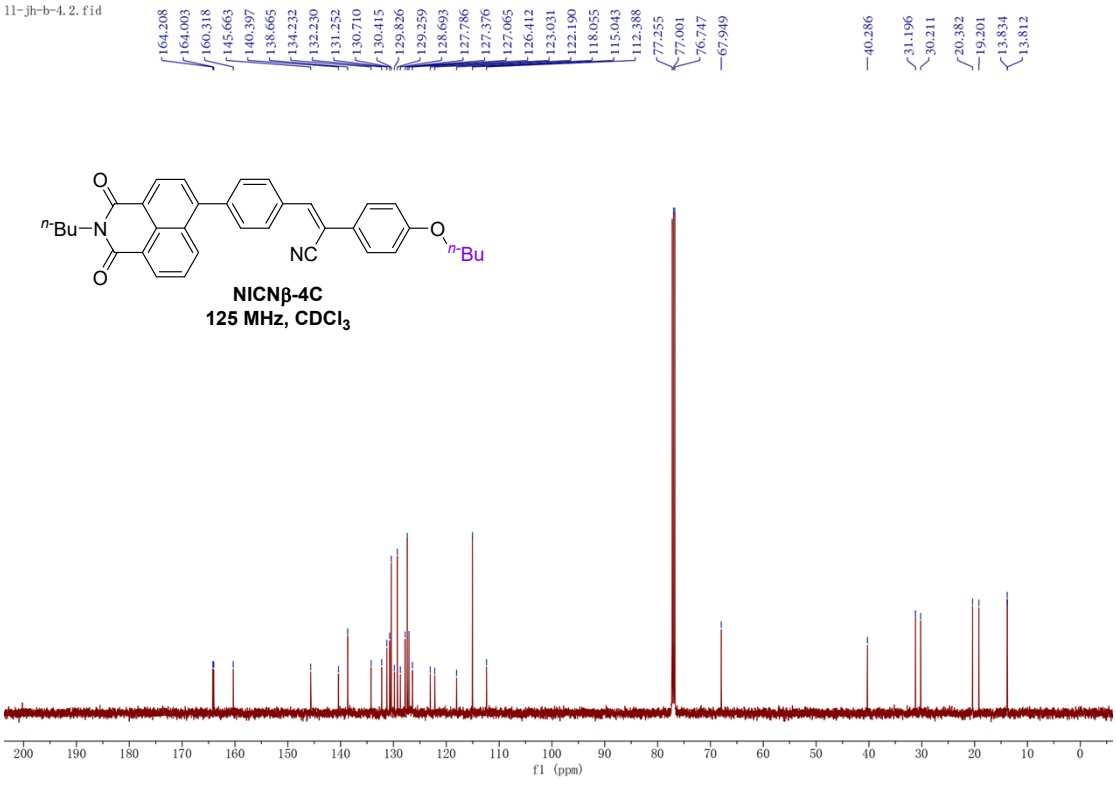
11-jh-b-4.2.fid
164.208
164.003
160.318
145.663
140.397
138.665
134.232
132.230
131.252
130.710
130.415
129.826
129.259
128.693
127.786
127.376
127.065
126.412
123.031
122.190
118.055
115.043
112.388
77.255
77.001
76.747
67.949
40.286
31.196
30.211
20.382
19.201
13.834
13.812
O
n-Bu–N
O
NC
O
n-Bu
NICNβ-4C
125 MHz, CDCl3
200
190
180
170
160
150
140
130
120
110
100
90
80
70
60
50
40
30
20
10
0
f1 (ppm)

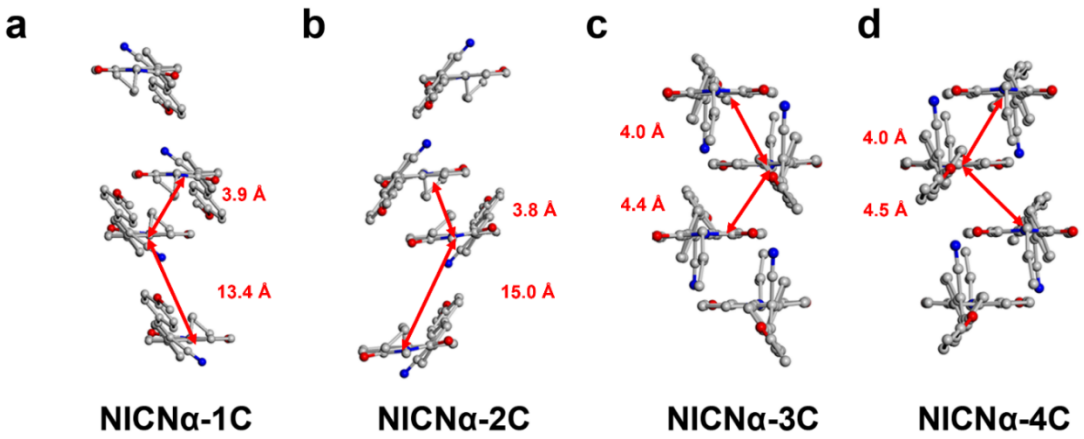

Figure S1. The crystalline structures and interlayer distances (the center distances between NI moieties) of NICNα-1C, NICNα-2C, NICNα-3C and NICNα-4C.

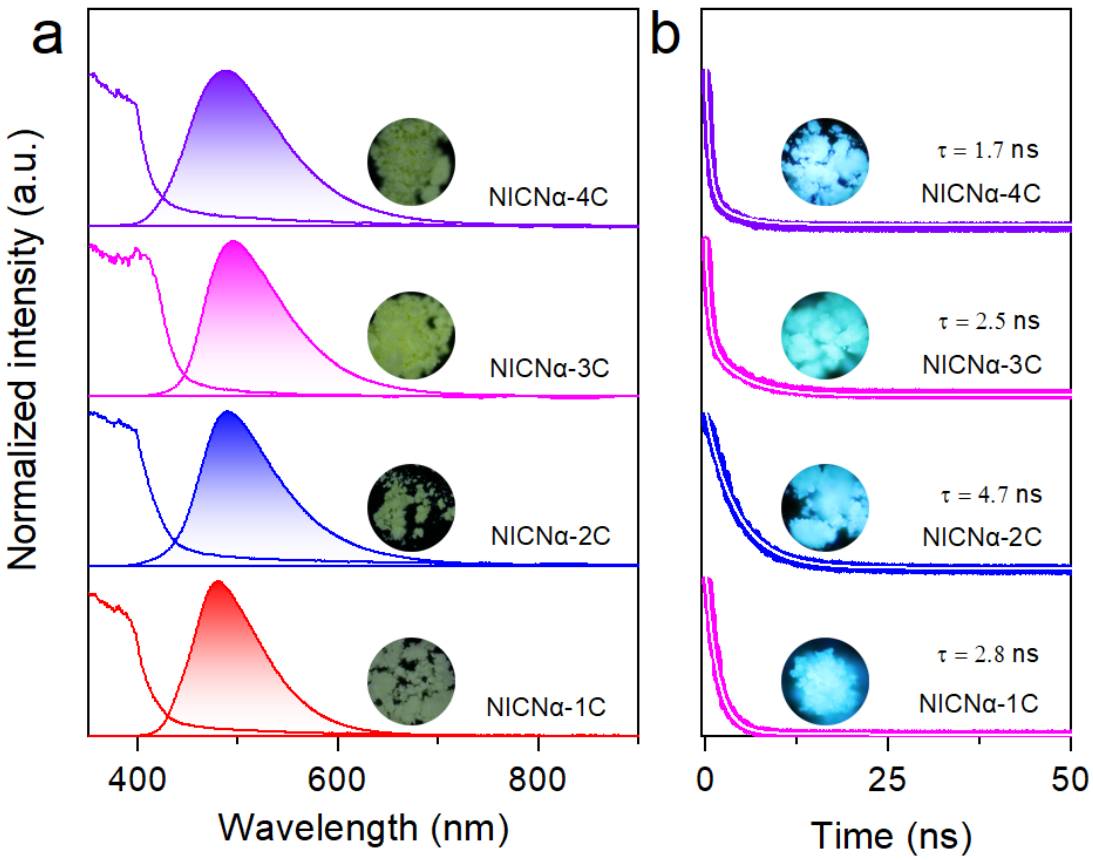

Figure S2. (a) The ambient PL emission and absorption spectra of NICNα-R (R = 1C, 2C, 3C and 4C). The insets illustrate the optical micrographs of corresponding sample. (b) The PL lifetime measurements of NICNα-R (R = 1C, 2C, 3C and 4C). The insets exhibit the PL micrographs of corresponding sample.

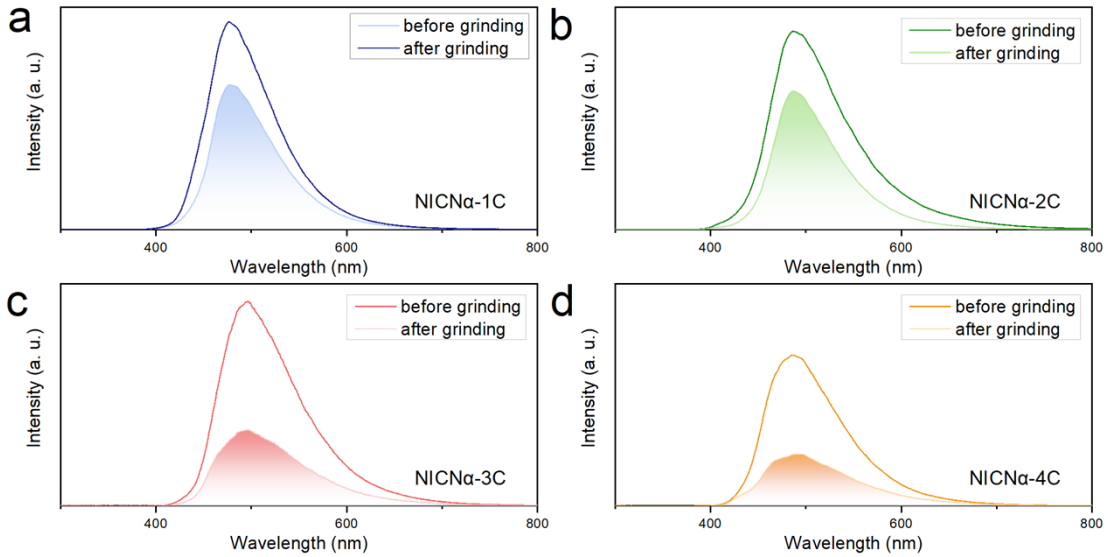

Figure S3. The comparisons of the emission spectra of (a) NICNα-1C, (b) NICNα-2C, (c) NICNα-3C and (d) NICNα-4C before and after grinding.

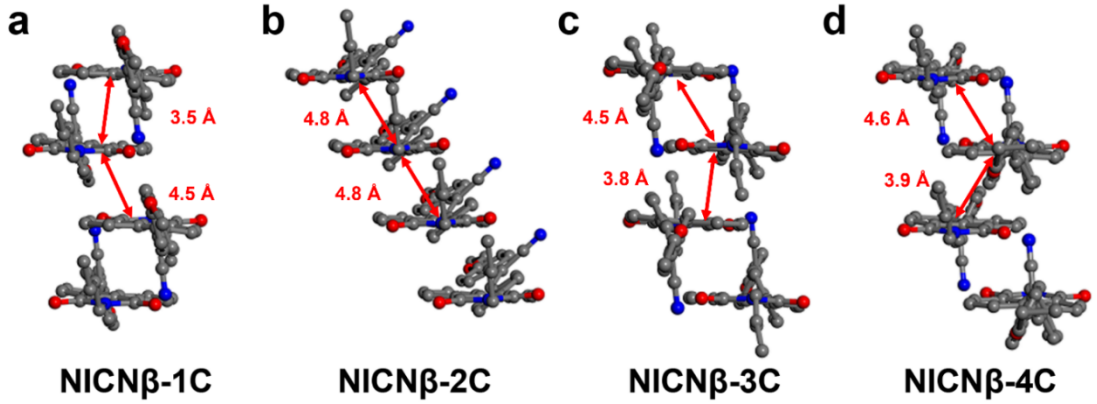

Figure S4. The crystalline structures and interlayer distances (the center distances between NI moieties) of NICNβ-1C, NICNβ-2C, NICNβ-3C and NICNβ-4C.

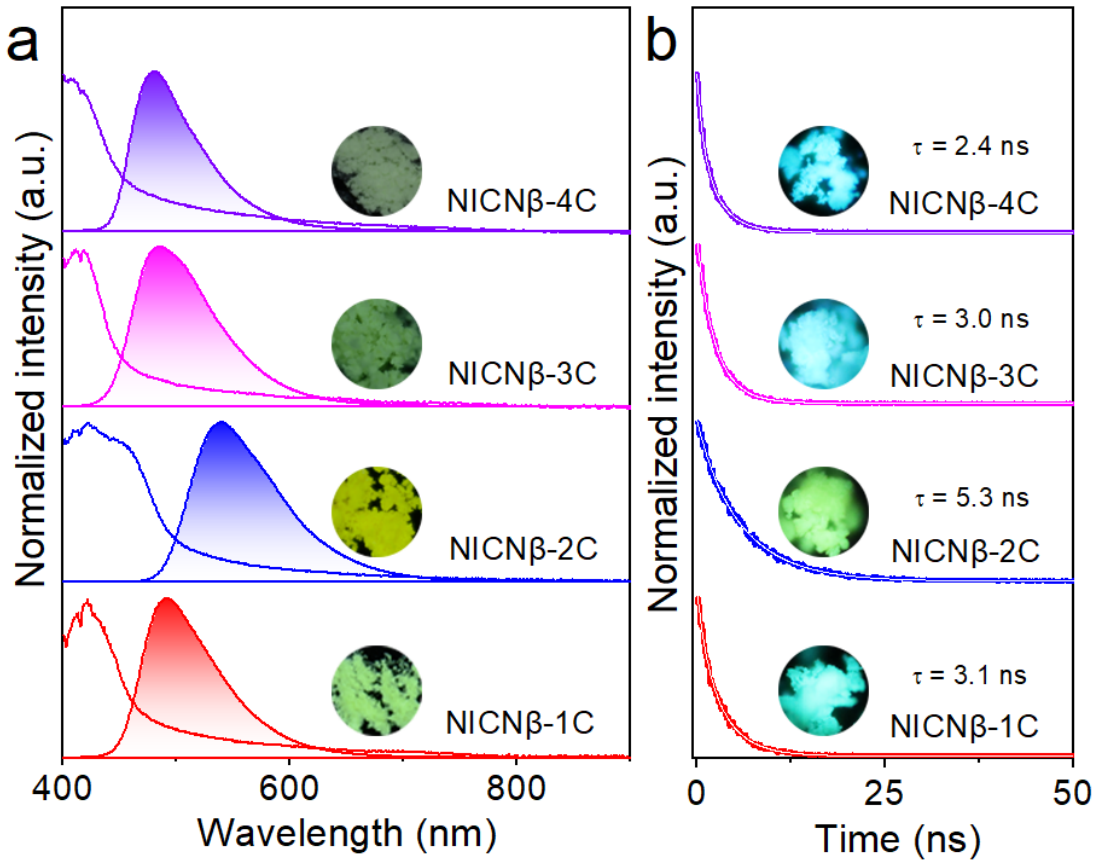

Figure S5. (a) The PL emission and absorption spectra of NICNβ-R (R = 1C, 2C, 3C and 4C) at ambient conditions. The insets illustrate the optical micrographs of corresponding sample. (b) The PL decay curves of NICNβ-R (R = 1C, 2C, 3C and 4C). The insets exhibit the PL micrographs of corresponding sample.

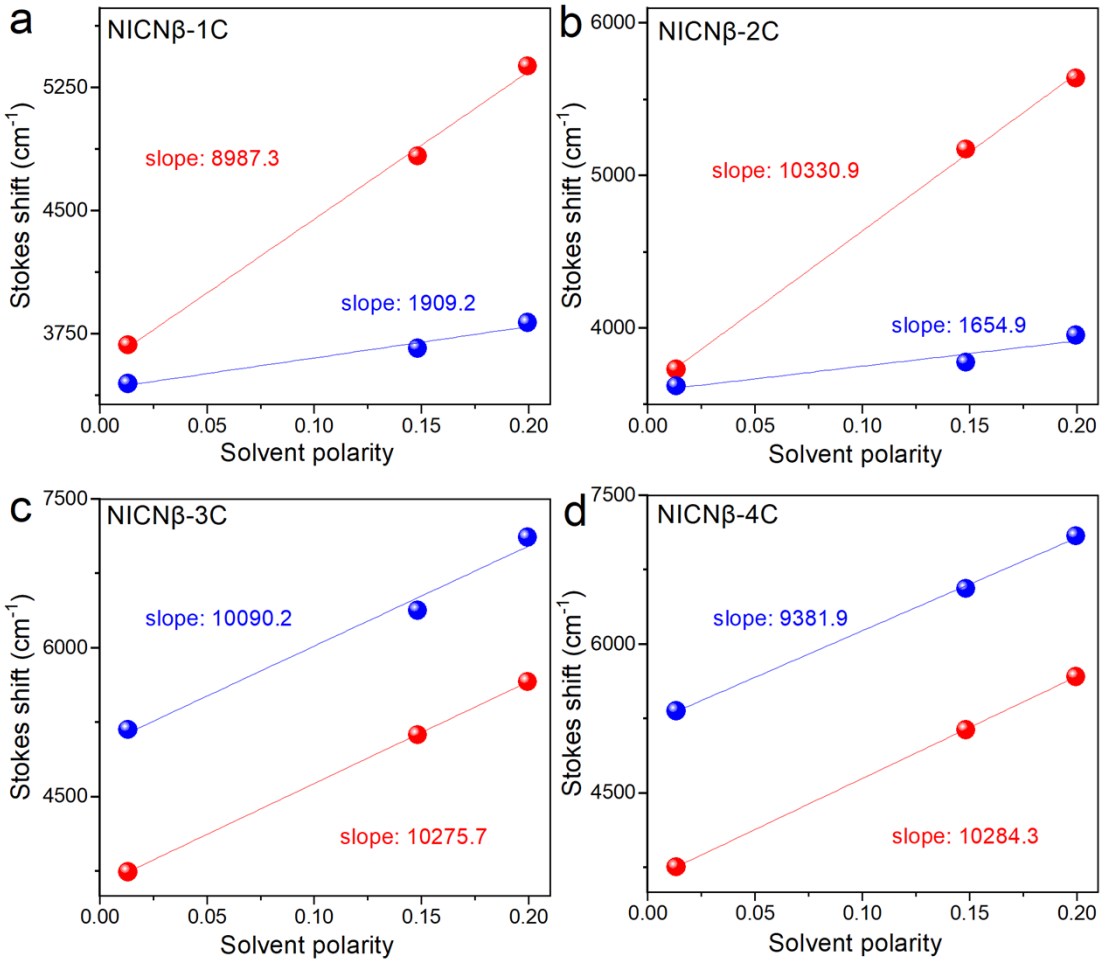

Figure S6. The Stokes shifts of (a) NICNβ-1C, (b) NICNβ-2C, (c) NICNβ-3C and (d) NICNβ-4C in differnt solvents.

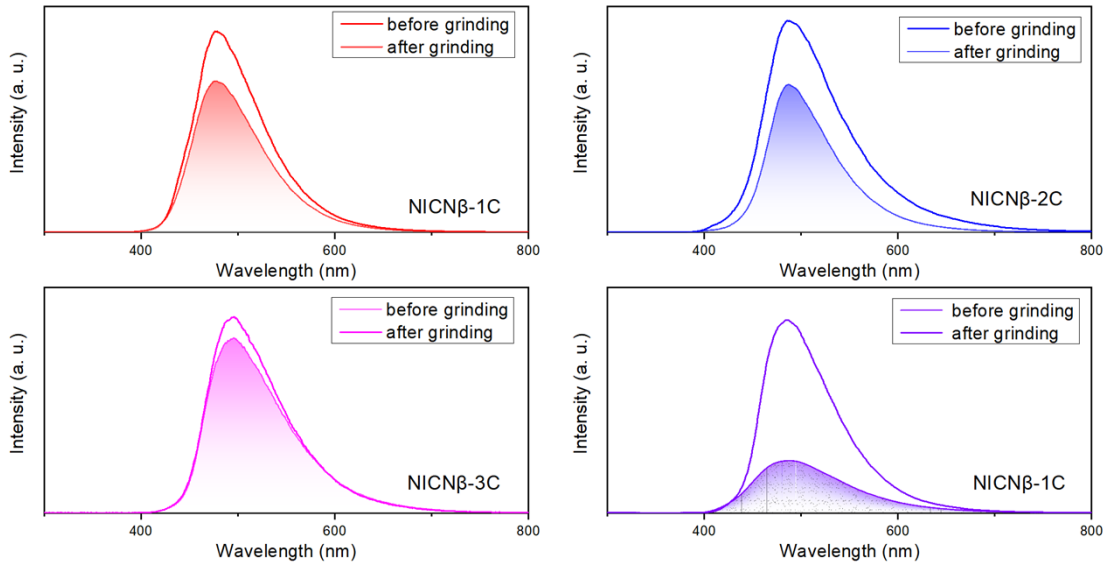

Figure S7. The PL emission spectra of (a) NICNβ-1C, (b) NICNβ-2C, (c) NICNβ-3C and (d) NICNβ-4C before and after grinding.

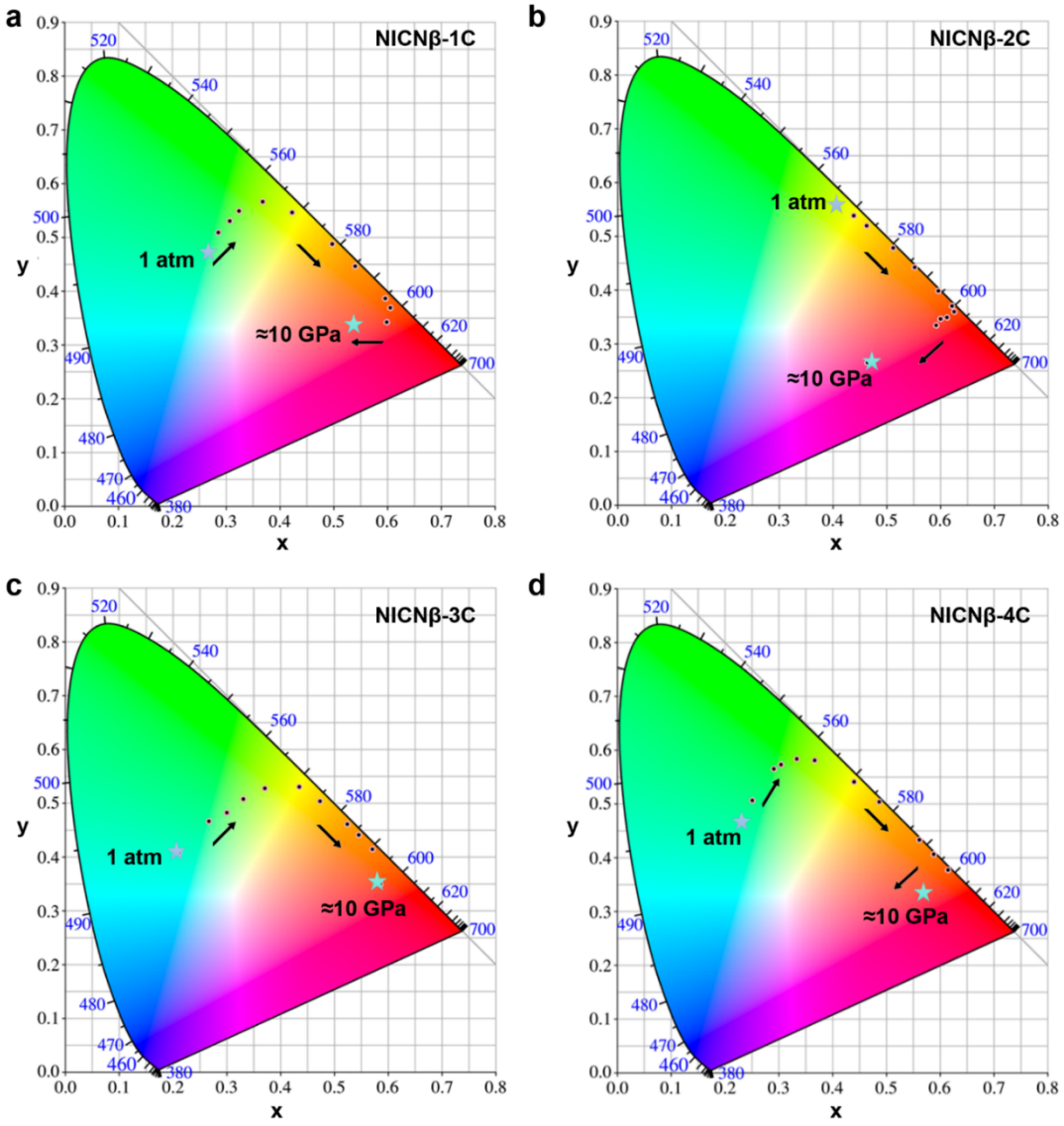

Figure S8. The pressure-dependent CIE chromaticity coordinate of (a) NICNβ-1C, (b) NICNβ-2C, (c) NICNβ-3C and (d) NICNβ-4C.

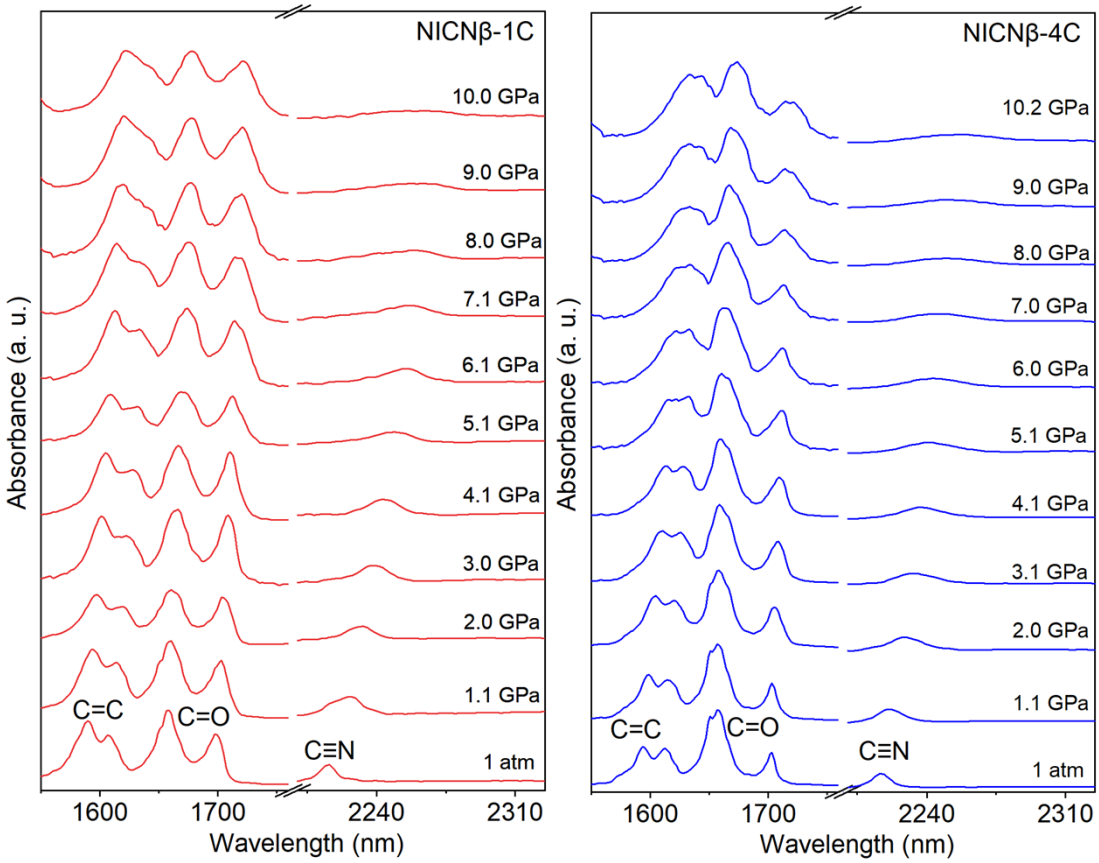

Figure S9. Selected IR spectra of (a) NICNβ-1C and (b) NICNβ-4C with increasing pressure to ≈10 GPa.

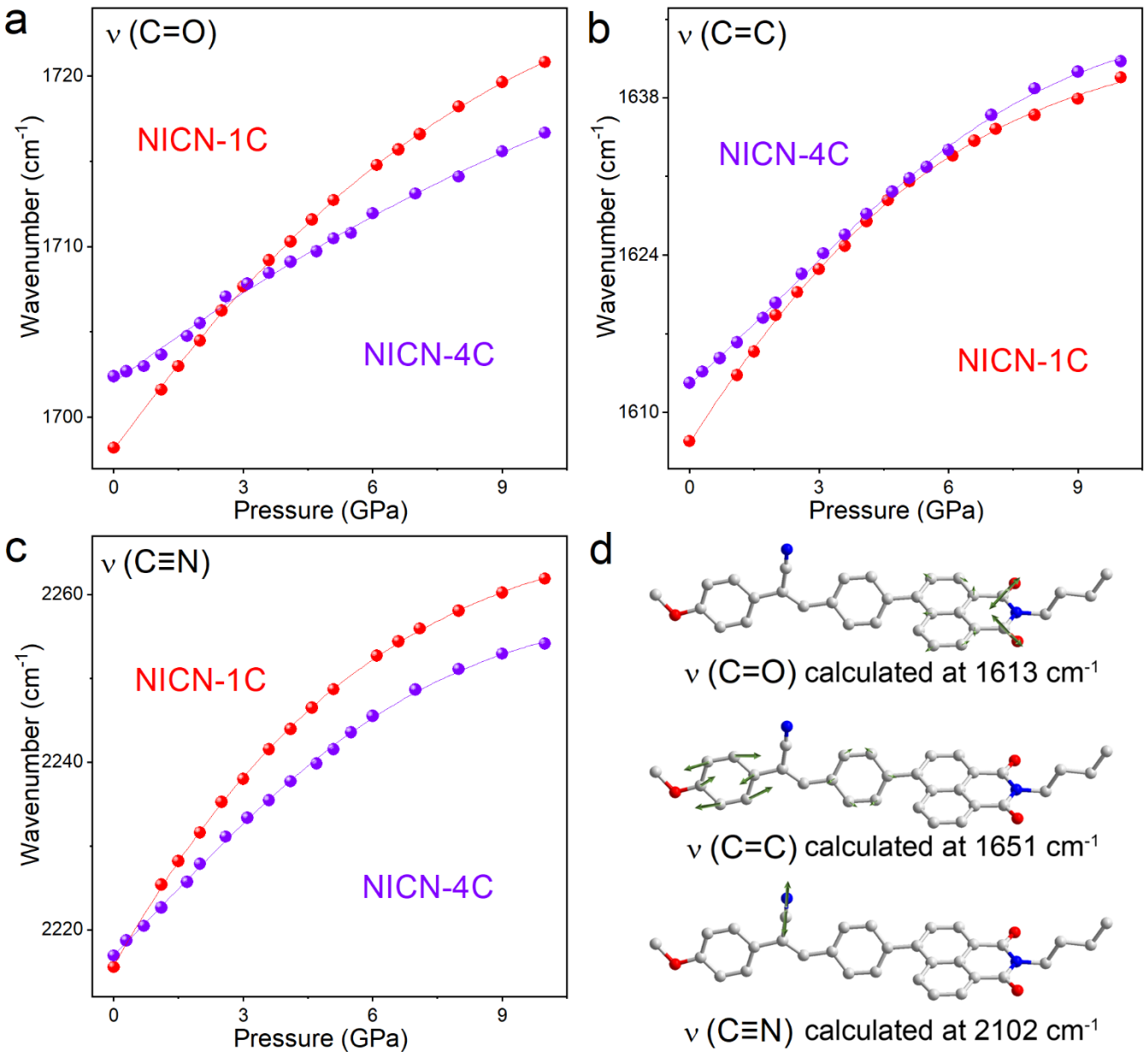

Figure S10. Comparisons of the wavelengths of selected IR modes of (a) C=O, (b) C=C and (c) C≡N at high pressure. (d) The illustration of corresponding vibration modes.

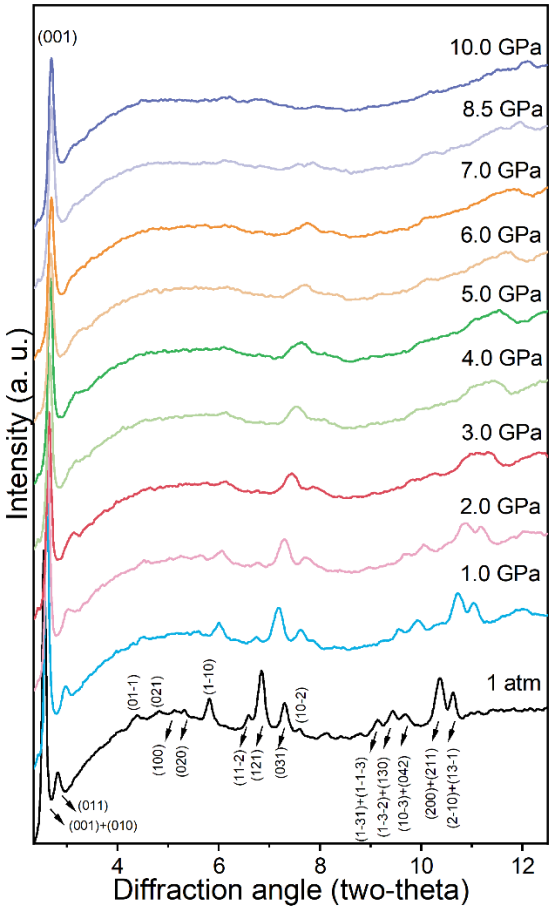

Figure S11. The ADXRD patterns of NICSβ-4C with increasing pressure.

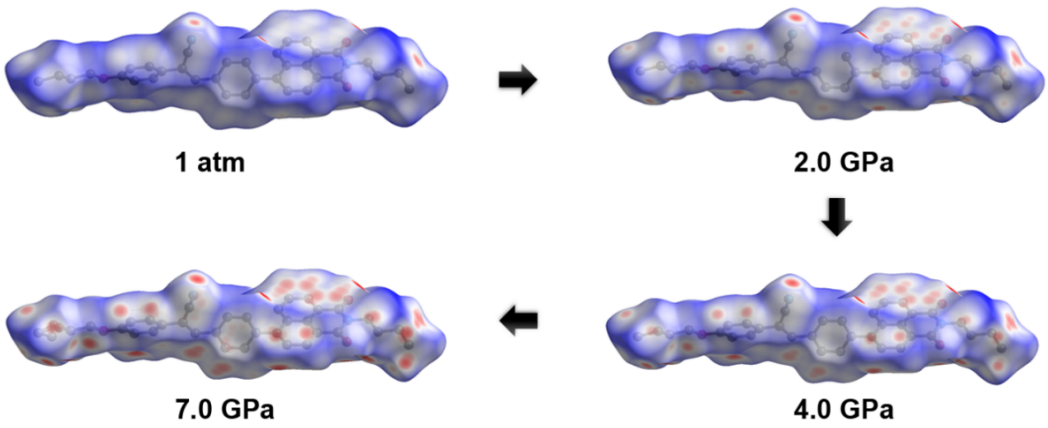

Figure S12. The Hirshfeld surface of NICNβ-4C molecule at selected pressures.

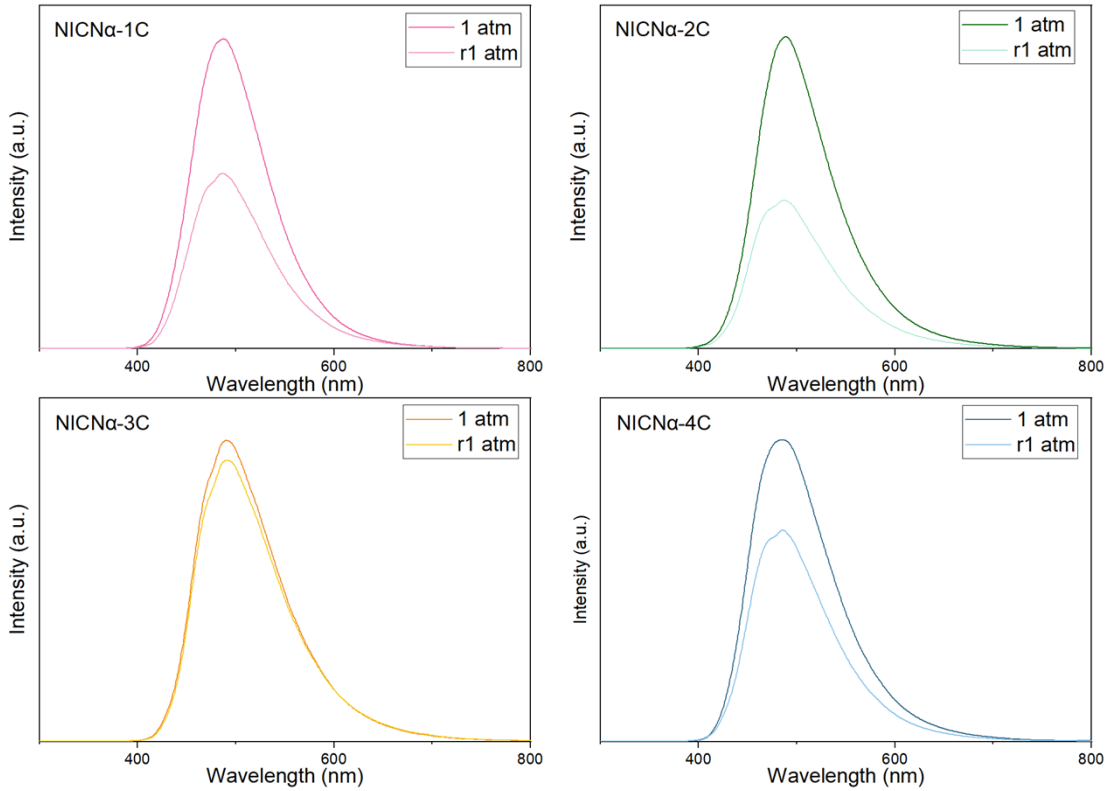

Figure S13. Emission spectra under ambient conditions and recovered emission spectra after high-pressure compression of NICNα-R.

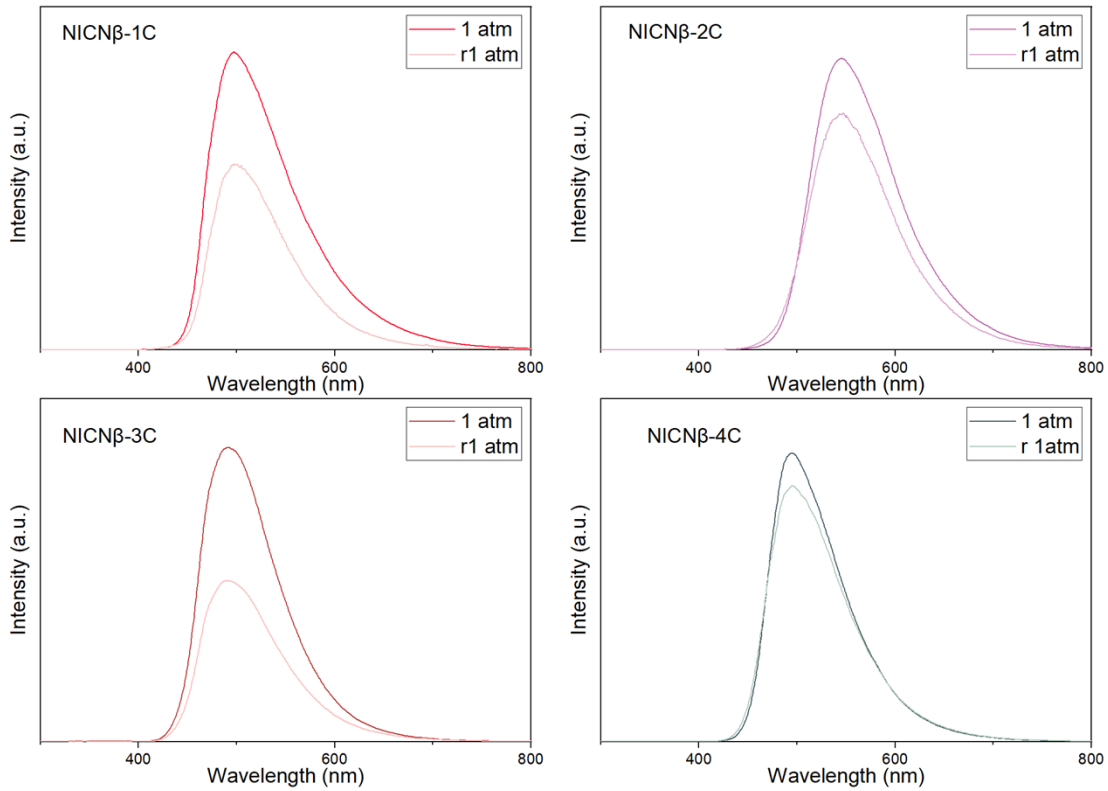

Figure S14. Emission spectra under ambient conditions and recovered emission spectra after high-pressure compression of NICNβ-R.

Reference

1. Y. Ni, L. Yang, L. Kong, C. Wang, Q. Zhang and J. Yang, Highly efficient dual-state emission and two-photon absorption of novel naphthalimide functionalized cyanostilbene derivatives with finely tuned terminal alkoxyl groups, *Mater. Chem. Front.*, 2022, **6**, 3522-3530.

2. J.-F. Luo, B.-C. Tang, C.-X. Gao, M. Li, Y.-H. Han and G.-T. Zou, Effects of high pressure on the Raman and fluorescence emission spectra of two novel 1,3,4-oxadiazole derivatives, *Chin. Phys.*, 2005, **14**, 1770.

3. H. Yuan, K. Wang, K. Yang, B. Liu and B. Zou, Luminescence properties of compressed tetraphenylethene: the role of intermolecular interactions, *J. Phys. Chem. Lett.*, 2014, **5**, 2968-2973.

4. X. Wang, Q. Liu, H. Yan, Z. Liu, M. Yao, Q. Zhang, S. Gong and W. He, Piezochromic luminescence behaviors of two new benzothiazole-enamido boron difluoride complexes: intra- and inter-molecular effects induced by hydrostatic compression, *Chem. Commun.*, 2015, **51**, 7497-7500.

5. Y. Zhang, Q. Song, K. Wang, W. Mao, F. Cao, J. Sun, L. Zhan, Y. Lv, Y. Ma, B. Zou and C. Zhang, Polymorphic crystals and their luminescence switching of triphenylacrylonitrile derivatives upon solvent vapour, mechanical, and thermal stimuli, *J. Mater. Chem. C*, 2015, **3**, 3049-3054.

6. X. Meng, G. Qi, X. Li, Z. Wang, K. Wang, B. Zou and Y. Ma, Spiropyran-based multi-colored switching tuned by pressure and mechanical grinding, *J. Mater. Chem. C*, 2016, **4**, 7584-7588.

7. Y. Zhang, M. Qile, J. Sun, M. Xu, K. Wang, F. Cao, W. Li, Q. Song, B. Zou and C. Zhang, Ratiometric pressure sensors based on cyano-substituted oligo(*p*-phenylene vinylene) derivatives in the hybridized local and charge-transfer excited state, *J. Mater. Chem. C*, 2016, **4**, 9954-9960.

8. S. Zhang, Y. Dai, S. Luo, Y. Gao, N. Gao, K. Wang, B. Zou, B. Yang and Y. Ma, Rehybridization of nitrogen atom induced photoluminescence enhancement under pressure stimulation, *Adv. Funct. Mater.*, 2017, **27**,1602276.

9. Y. Li, Z. Ma, A. Li, W. Xu, Y. Wang, H. Jiang, K. Wang, Y. Zhao and X. Jia, A single crystal with multiple functions of optical waveguide, aggregation-induced emission, and mechanochromism, *ACS Appl. Mater. Interfaces*, 2017, **9**, 8910-8918.

10. A. Li, N. Chu, J. Liu, H. Liu, J. Wang, S. Xu, H. Cui, H. Zhang, W. Xu and Z. Ma, Pressure-induced remarkable luminescence switch of a dimer form of donor–acceptor–donor triphenylamine (TPA) derivative, *Mater. Chem. Front.*, 2019, **3**, 2768-2774.

11. M. Wu, H. Liu, H. Liu, T. Lu, S. Wang, G. Niu, L. Sui, F. Bai, B. Yang, K. Wang, X. Yang and B. Zou, Pressure-induced restricting intermolecular vibration of a herringbone dimer for significantly enhanced multicolor emission in rotor-free truxene crystals, *J. Phys. Chem. Lett.*, 2022, **13**, 2493-2499.

12. Y. Dai, H. Liu, T. Geng, R. Duan, X. Li, Y. Liu, W. Liu, B.-G. He, L. Sui, K. Wang, B. Zou, B. Yang and Y. Qi, Piezochromic fluorescence of anthracene derivative crystals with different stacking patterns designed around excimers, *J. Mater. Chem. C*, 2023, **11**, 4892-4898.